

LWS-spectroscopy of Herbig Haro objects and molecular outflows in the Cha II dark cloud^{*}

B. Nisini¹, D. Lorenzetti², M. Cohen³, C. Ceccarelli^{1,4}, T. Giannini¹, R. Liseau^{1,5}, S. Molinari^{1,6}, A. Radicchi¹, P. Saraceno¹, L. Spinoglio¹, E. Tommasi¹, P.E. Clegg⁷, P.A.R. Ade⁷, C. Armand⁶, M.J. Barlow⁸, M. Burgdorf⁶, E. Caux⁹, P. Cerulli¹, S.E. Church¹⁰, A. Di Giorgio⁶, J. Fischer¹¹, I. Furniss⁸, W.M. Glencross⁸, M.J. Griffin⁷, C. Gry⁶, K.J. King¹², T. Lim⁶, D.A. Naylor¹³, D. Texier⁶, R. Orfei¹, Nguyen-Q-Rieu¹⁴, S. Sidher⁶, H.A. Smith¹⁵, B.M. Swinyard¹², N. Trams⁶, S.J. Unger¹², and G.J. White⁷

¹ CNR-Istituto di Fisica dello Spazio Interplanetario, Casella Postale 27, I-00044 Frascati, Italy

² Osservatorio Astronomico di Roma, I-00040 Monte Porzio, Italy

³ Radio Astronomy Laboratory, Univ. of California, Berkeley, USA

⁴ Laboratoire d'Astrophysique de l'Observatoire de Grenoble, rue de la Piscine, BP 53, F-38041 Grenoble, France

⁵ Stockholm Observatory, S-133 36 Saltsjöbaden, Sweden

⁶ The LWS Instrument-Dedicated Team, ISO Science Operations Centre, Villafranca, Spain

⁷ Physics Department, Queen Mary & Westfield College, University of London, Mile End Road, London E1 4NS, UK

⁸ University College London, Dept. of Physics and Astronomy, Gower Street, London WC1E 6BT, UK

⁹ CESR/CNRS-UPS, BP 4346, F-31029 Toulouse Cedex, France

¹⁰ California Institute of Technology, Pasadena, CA 91125, USA

¹¹ Naval Research Laboratory, Remote Sensing Division, 4555 Overlook Ave., SW Washington D.C., USA

¹² Space Science Department, Rutherford Appleton Lab, Chilton, Oxon OX11 0QX, UK

¹³ Dept. of Physics, University of Lethbridge - Lethbridge, Alberta T1K 3M4, Canada

¹⁴ Observatoire de Paris, 61 avenue de l'Observatoire, F-75014 Paris, France

¹⁵ Laboratory for Astrophysics, National Air and Space Museum, Smithsonian Institution, Washington D.C., USA

Received 28 June 1996 / Accepted 13 September 1996

Abstract. We present the first far infrared spectra of the Herbig Haro objects HH 52-53-54 and of IRAS 12496-7650, all located in the nearby star forming region known as Chamaleon II dark cloud, obtained with the Long Wavelength Spectrometer (LWS) onboard the Infrared Space Observatory (ISO). The richest spectrum is found in HH54, showing molecular transitions (CO with J_u from 19 to 14, water vapour mainly in its ortho form and OH) and low excitation fine structure lines ([OI]63, 145 μm , [CII]158 μm). In HH52 and HH53, only the [OI] and [CII] lines are detected. The LWS spectrum of IRAS 12496-7650 shows both fine structure and CO lines. The [CII]158 μm line is ubiquitous in the region, as proved by its presence in all ISO pointings, including the raster scan maps. The fine structure lines are used to evaluate the physical parameters of the emitting regions. In particular, the mass loss rates of each outflow present in the region, are derived from the [OI]63 μm line luminosity.

Key words: stars: formation – stars: individual: IRAS 12496-7650 – ISM: jets and outflows – ISM: individual objects: HH52,53,54 – infrared: ISM: lines

1. Introduction

The Cha dark clouds constitute one of the nearest star-forming complexes to the Sun. Three distinct regions appear contiguous on the sky : Cha I, II, III. Of these three, Cha I and II are known to contain young stellar objects (YSOs), while Cha III is not (Henning & Thamm 1994). Cha II is thought to represent an earlier evolutionary state than Cha I (Gauvin & Strom 1992). During his H_α emission survey of these clouds, Schwartz (1977) discovered several new Herbig-Haro objects (HHs). The focus of our ISO LWS observations is the group HH 52-53-54 and the IRAS source 12496-7650, that lies some 14'' to their SW, and has been regarded by some (*e.g.* Cohen & Schwartz 1987; Hughes et al. 1989) as their exciting star. Our primary interest is the far-infrared (FIR) emission line spectrum of these HHs and of the vicinity of 12496-7650, because of the diagnostic potential of these lines for understanding the excitation mechanisms

Send offprint requests to: B.Nisini, bruni@taurus.ifs.i.fra.cnr.it

^{*} Based on observations with ISO, an ESA project with instruments funded by ESA Member States and with the participation of ISAS and NASA

Table 1. Journal of observations

Source	Date	# orbit	$\alpha(1950)$			$\delta(1950)$			raster points (step size)	t_{int} (sec)	n_s
			<i>h</i>	<i>m</i>	<i>s</i>	<i>o</i>	<i>'</i>	<i>''</i>			
HH 52	17 Feb	92	12	51	28.0	-76	41	34.9	-	6.0	15
HH 53A	17 Feb	92	12	51	36.2	-76	41	12.0	-	6.0	15
HH 54B	17 Feb	92	12	52	10.6	-76	40	04.0	-	6.0	15
IRAS12496-7650	11 Mar	115	12	49	38.0	-76	50	45.0	-	7.6	19
IRAS12496-7650 flow	11 Mar	115	12	49	45.4	-76	50	33.0	3×3 (100'')	0.45	3
HHs flow	11 Mar	115	12	51	27.6	-76	41	52.0	3×3 (100'')	0.45	3

Notes: t_{int} = integration time per spectral sample, n_s = number of spectral scans.

Table 2. Observed line intensities

λ (obs.) (μm)	Line ident.	HH54	HH53	HH52	HHs flow	IRAS 12496	IRAS 12496 flow
$F \pm \Delta F^\dagger$ ($10^{-19} W cm^{-2}$)							
63.2	[OI]	14.2 ± 0.07	4.13 ± 0.33	4.97 ± 0.23		4.49 ± 0.27	
113.4	o-H ₂ O	0.32 ± 0.06					
119.4	OH	0.48 ± 0.06					
137.1	CO 19-18	$0.22 \pm 0.1^*$					
138.7	p-H ₂ O	$0.34 \pm 0.1^*$					
144.8	CO 18-17	$0.31 \pm 0.04^*$					
145.5	[OI]	$0.71 \pm 0.06^*$	0.20 ± 0.05	0.15 ± 0.05		0.31 ± 0.07	
153.2	CO 17-16	0.35 ± 0.05				0.67 ± 0.07	
157.7	[CII]	0.80 ± 0.04	0.74 ± 0.07	0.79 ± 0.06	0.84 ± 0.13	0.43 ± 0.08	0.47 ± 0.09
162.8	CO 16-15	0.53 ± 0.04				0.26 ± 0.09	
173.7	CO 15-14	$0.58 \pm 0.05^*$				0.89 ± 0.09	
174.7	o-H ₂ O	$0.24 \pm 0.05^*$					
179.6	o-H ₂ O	1.20 ± 0.11					
185.9	CO 14-13	1.37 ± 0.24					

Notes: † 1σ statistical errors, * lines deblended with a two gaussian fit.

and origin of HHs. There is precedent in that Cohen et al. (1988) have observed strong $63 \mu m$ [OI] emission lines in a number of northern HHs from the Kuiper Airborne Observatory (KAO).

Optically, HH 52 and 53 each consist of three dominant knots embedded in diffuse nebulosity, elongated roughly east-west, and extending some $40 \times 15''$ (Schwartz 1977; Sandell et al. 1987). HH 54, however, appears as a complex of about ten knots, some $40''$ in diameter. Images in the S(1) 1-0 line of molecular hydrogen (Sandell et al. 1987; Gredel 1994) reveal essentially the same structure. Infrared searches for the exciting stars of HH 52-54 have likewise yielded indefinite results. The $2 \mu m$ candidates of Reipurth & Wamsteker (1983) and Sandell et al. (1987) can be excluded on the grounds of IR colors, location, and the absence of any reversals of HH velocity field in their vicinities. No KAO candidates were found at 50 or $100 \mu m$ (Cohen et al. 1984) but several IRAS sources are found in this part of the Cha II cloud: IRAS 12515-7641, 12522-7640, and 12496-7650.

Knee (1992) associates a CO bipolar flow with 12515-7641 suggesting this source as the exciting star of HH54 and HH53. HH 54 seems to be associated with a monopolar blue-shifted CO flow (Knee 1992), perhaps driven by an Alfvénic wind from another low-mass embedded YSO (12522-7640). In the years before Knee's (1992) critical CO survey, the relative brightness of 12496-7650 (the third of the IRAS candidate excit-

ing stars), compared with 12515-7641 and 12522-7640, and its rough alignment with the axis HH 54-53-52, caused Cohen & Schwartz (1987) to suggest that this object might drive all these HHs. IRAS12496-7650 is the only known intermediate mass YSO in Cha II. It has continued to undergo irregular and significant near-infrared variations whose amplitude decreases with wavelength. It is a probable deeply embedded Herbig Ae star around which dusty clumps circulate, irregularly obscuring the starlight (Hughes et al. 1991). Knee (1992) finds a weak bipolar CO flow associated with 12496-7650 and argues that the strong CO line wings observed near this source are in no way connected with those seen around HH 52-54. IRAS 12496-7650 is, thus, an outflow YSO but is apparently not responsible for these HHs.

2. Observations and results

We observed the regions of HH 52-53-54 and of IRAS 12496-7650 with the ISO (Kessler et al. 1996) LWS instrument (Clegg et al. 1996) in grating mode ($43\text{-}196.7 \mu m$, $R \sim 200$). The journal of observations is given in Table 1. We targeted HH 54B, HH 53A, HH 52 and IRAS 12496-7650 and made 3×3 maps covering the two CO associated outflows. The spectrum is over-sampled by a factor 4 and each spectral sample is integrated for a total time t_{int} given in Table 1. A spectrum is composed of

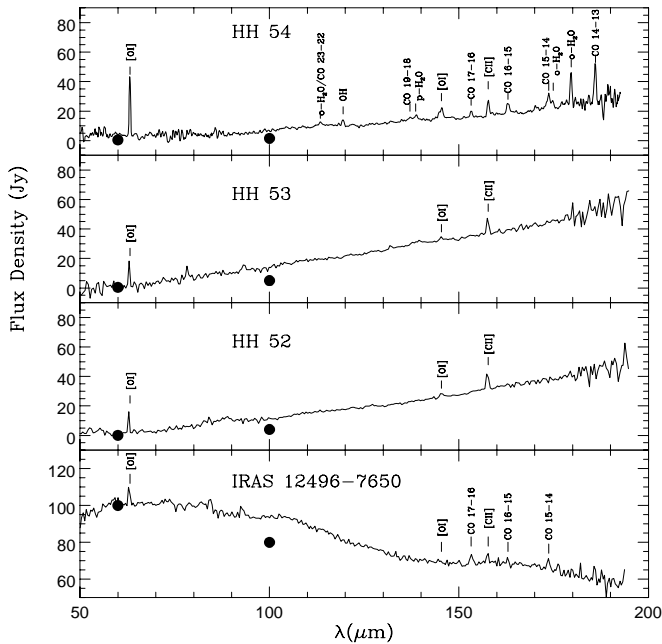


Fig. 1. LWS spectra of HH 54, HH 52, HH 53 and IRAS 12496-7650. The spectra have been rebinned at $\Delta\lambda = 0.4 \mu\text{m}$. Filled dots are the fluxes (ADDSCAN, Cohen & Schwartz, 1987) of the IRAS sources present in the beam: IRAS 12522-7640 in the beam of HH 54 and IRAS 12515-7641 in the beams of HH 52 and 53.

ten sub-spectra corresponding to the ten detectors. The single scans of each sub-spectrum have been flux calibrated using observations of Uranus. Deglitching of individual scans (made necessary by cosmic ray impacts) was done by removing values above two times the median of all scans. The scans obtained were then averaged together and corrected for low-frequency baseline fringes (Swinyard et al. 1996). The spectra from each detector were re-scaled to the average of the overlapping portions. From this procedure we estimate a flux calibration accuracy of $\sim 30\%$.

The resulting spectra are presented in Fig. 1 where the fluxes of the IRAS point sources present in the beam are also reported. Agreement with the IRAS fluxes is to within the calibration accuracy.

We do not detect any line in the single spectra of each raster maps. All the spectra of each map have been therefore averaged together to obtain an *off*-position spectrum whose total integration time is comparable to the *on*-position.

In Table 2, we list the transitions identified in the spectra together with their integrated intensities, computed by gaussian fitting the measured profile. When lines are observed by two different detectors, the two flux determinations are always inside the calibration accuracy.

3. Discussion

Since the [CII]158 μm line is detected both in the observed sources and in the integrated spectra along the associated flow

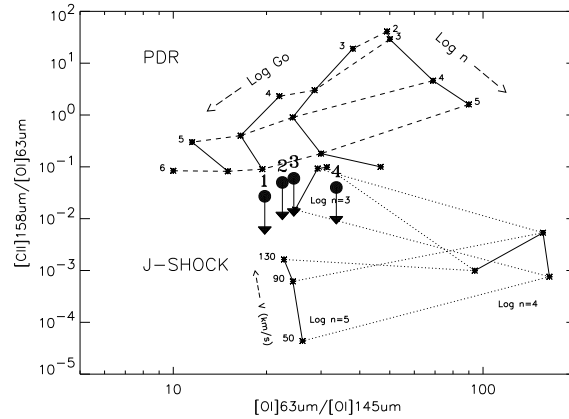


Fig. 2. The [OI]63 μm /[OI]145 μm and [CII]158 μm /[OI]63 μm ratios are plotted as a function of different emitting conditions. For the PDR, we plot the model results by Wolfire et al. (1990), while for J-shock the model of Hollenbach & McKee (1989) is reported. The sources are labelled as (1) for HH54, (2) for HH53, (3) for HH52 and (4) for IRAS 12496

(appearing at comparable flux levels in all the observed positions, about $8 \times 10^{-20} \text{ W cm}^{-2}$ around the HHs and $4 \times 10^{-20} \text{ W cm}^{-2}$ around the IRAS source), we infer that the [CII] emission is not intrinsic to the HHs or to the IRAS source. Such a uniform distribution of the [CII] emission attests to its photodissociation origin. The observed flux density is consistent with a weak FUV field, comparable with the average interstellar field, illuminating a relatively low density region (Hollenbach et al., 1991).

[OI] emission, on the contrary, is observed only toward the HHs and IRAS12496. [OI] is a good tracer of fast shock emission and potentially it can be used to detect shocks deeply embedded in the cloud, not observable by other visible and near-infrared tracers. The non detection of [OI] emission in the flows implies that the only shocked regions in the observed field are those traced by the HHs.

Among the three HH objects, HH 54 is the source showing the richest far-infrared spectrum, dominated, in addition to [OI], by CO and H₂O lines, indicating low-excitation conditions (Liseau et al. 1996). Toward HH 52 and HH 53 only the [OI] lines at 63 and 145 μm were detected. The observed differences among the three spectra are probably due to differing filling factors, rather than to a real difference in the excitation conditions. Indeed, while optically the three HH objects show similar excitations, the HH54 knots appear three times more extended than HH52 and HH53 (Sandell 1987).

In IRAS 12496 we detected the two [OI] lines together with CO rotational lines from $J_u = 17$ to 15, also indicating low-excitation conditions.

The observed [OI] lines and the upper limits on the [CII] 158 μm line, obtained by subtracting the *off* from the *on*-source spectra and taking three times the rms noise of the so obtained spectrum, can be used to infer some properties of the emitting conditions. Fig. 2 shows the observed ratios as compared with

Table 3. Mass loss rates

Source	$\dot{M}([\text{OI}]63\mu\text{m})$ $10^{-6}M_{\odot}/\text{yr}$	$\dot{M}(\text{CO})$ $10^{-6}M_{\odot}/\text{yr}$
HH 54	2.6	1.0
HH 52	1.0	1.2
HH 53	0.8	1.2
IRAS12496	0.9	..

a model of photodissociation (Wolfire et al. 1990) and with the J-shock models of Hollenbach & McKee (1989); the observed ratios are consistent with shock emission in all the sources. Liseau et al., analyzing the CO and water lines in HH54, derived a pre-shock density of $\sim 2 \cdot 10^3 \text{ cm}^{-3}$ and a temperature of $\sim 300 \text{ K}$. From the [OI] lines ratio alone we cannot infer if the [OI] emission comes from the same cold shocked region; in J shock models, however, it is expected that [OI] traces a warmer and faster shock component originating in the "wind"-shock.

The three CO lines detected in IRAS12496 do not show any decrement, indicating that we are probably observing the peak of the CO line intensity distribution. Assuming an H_2 density of $\sim 10^5$, the distribution peaks at $J \sim 17$ for a gas temperature of $\sim 1000 \text{ K}$ (McKee et al. 1982); in this case, the molecular gas in the IRAS source would be warmer than in these HH.

For temperatures greater than 300 K, the [OI] $63\mu\text{m}$ line is always optically thin providing that the hydrogen column density is less than $1 \cdot 10^{23} \text{ cm}^{-2}$. This is likely the case in HH54, where the CO model fit indicates $N(\text{H}_2) = 5 \cdot 10^{20} \text{ cm}^{-2}$ for the cold gas and Gredel (1994) estimates a column density of $3.6 \cdot 10^{17}$ for the warm H_2 . In HH54 the cooling due to the [OI] $63\mu\text{m}$ line alone, assuming a distance of 250 pc, is $3 \cdot 10^{-2} L_{\odot}$, which is comparable with the cooling of the molecular lines in the cold shock region.

Given these conditions, *i.e.* the $63\mu\text{m}$ line optically thin and providing the major cooling in the fast shock region, the [OI] luminosity in HH54 can be used to derive the mass loss rate associated with the flow, adopting the relationship $L(63\mu\text{m})/L_{\odot} = 0.1 \dot{M}/10^{-5}M_{\odot}/\text{yr}$ given by Hollenbach (1985). Since the other HH objects appear to have the same excitation conditions, we have made separate estimates of the mass loss rates of the flows present in the region. We report the obtained values in Table 3, which lists also the \dot{M} measured from CO 1-0 (Knee, 1992), assuming a ratio between the CO flow velocity and the [OI] shock velocity of 0.2 (Hollenbach, 1985). While the $\dot{M}([\text{OI}]63\mu\text{m})$ derived for HH 52 and HH 53 is reasonably in agreement with that derived from CO, the [OI] in HH54B indicates a larger \dot{M} . The parameters of the compact outflow associated to HH54 appear difficult to define from the CO map, being confused with the more extended outflow; the [OI] probably provides a better determination of the \dot{M} value. Our derived values suggest that HH 54 and the other HH objects are not excited by the same source, being driven by winds of different intensities. IRAS 12496 shows a \dot{M} value comparable with that of HH 52 and HH53, therefore we cannot exclude, on this basis, that it can indeed excite these two HHs.

References

- Clegg P.E. et al. 1996, this volume
 Cohen M., Harvey P.M., Schwartz R.D., Wilking B.A. 1984, ApJ 278, 671
 Cohen M., Hollenbach D.J., Haas M.R., Erickson E.F. 1988, ApJ 329, 863
 Cohen M., Schwartz R. D. 1987, ApJ, 316, 311
 Gauvin L., Strom K.M. 1992, ApJ 385, 217
 Gredel R. 1994, AA 292, 580
 Henning Th., Thamm E. 1994, ApSpSci 212, 215
 Hollenbach D. 1985, *Icarus* 61, 36
 Hollenbach D., McKee C.F. 1989, ApJ 342, 306
 Hollenbach D., Takahashi, T., Tielens, A.G.G.M. 1991, ApJ 377, 192.
 Hughes J.D., Emerson J.P., Zinnecker H, Whitelock P.A. 1989 MN-RAS, 236, 117
 Hughes J.D., Hartigan P., Graham J.A., Emerson J.P., Marang F. 1991, AJ 101, 1013
 Kessler M. et al. 1996, this volume
 Knee L.B.G. 1992, AA 259, 283
 Liseau R. et al. 1996, this volume
 McKee C., Storey J.W.V., Watson D.M., Green S. 1982, ApJ 259, 647
 Reipurth B., Wamsteker W. 1983, AA 119, 14
 Sandell G., Zealey W.J., Williams P.M., Taylor K.N.R., Storey J.V. 1987, AA 182, 237
 Schwartz R. D. 1977, ApJS 35, 161
 Swinyard B. et al. 1996, this volume
 Wolfire M.G., Tielens A.G.G.M., Hollenbach D. 1990, ApJ 358, 116